Bulg. J. Phys. **46** (2019) 37–48

Investigation of Size Dependent Thermoluminescence Emission from Amorphous Silicon Quantum Dots

B. Mesfin, **T. Senbeta**
Department of Physics, Addis Ababa University, Addis Ababa, Ethiopia

Received: *22 November 2018*

Abstract. We studied the size dependent thermoluminescence emission from small amorphous silicon quantum dots using the model of interactive multiple traps system (IMTS). The model consists of two active electron traps having activation energies $E_1 = 0.65$ eV and $E_2 = 0.80$ eV, a thermally disconnected deep trap (TDDT), and a luminescent center. For quantum dots of diameters between 3–6 nm, numerical evaluations are carried out to generate the glow curve and determine relevant parameters such as the symmetry factor (μ_g) and the order of kinetics (b). It is observed that as the size of the quantum dots decrease, the intensity of the thermoluminescence signal increase, the glow peaks positions are almost independent of the size of dots, and the curves follow first-order kinetics ($\mu_g \rightarrow 0.42$ and $b \rightarrow 1$). In addition, the glow curves possess two peaks corresponding to the two active electron trap levels with the intensity due to E_2 being larger than that due to E_1. Furthermore, numerical analysis of the same quantum dots using the two-traps-one-recombination center model (no TDDT traps) shows that, unlike that obtained using the IMTS model, the glow curves seems to obey second-order kinetics ($\mu_g \rightarrow 0.52$ and $b \rightarrow 2$) and the peaks positions shift towards high temperature values with an increase in size of the dots. In addition, the numerical simulations enable us to determine how the concentration of carriers in the traps/center evolves as a function of temperature and quantum dots size.

PACS codes: 78.60.Kn, 78.56.Cd, 78.67.Hc

1 Introduction

Nanostructured materials provides unprecedented control over the optical, electrical, magnetic, and thermal properties of semiconductors and insulators due to quantum confinement effect [1,2]. For indirect band gap materials, the extremely reduced dimensions lead to a major spread of the wave vector in k-space, thus producing a relaxation of the moment selection rule and the possibility of zero-phonon direct radiative optical transitions [3–5]. Furthermore, the confinement

results to an increase of the overlap between electron and hole wave functions in k-space, thereby increasing the probability of radiative recombination and a decrease in the probability of nonradiative recombination. Accordingly, quantum confinement effect enables indirect band gap nanostructured materials to be viable candidates for potential applications as optoelectronics devices.

In the last decade, the emission of light from silicon nanostructures (NSs) has become a research topic of current interest due to its potential for applications in silicon-based optoelectronic devices [6, 7]. In particular, it has been found that amorphous silicon (a-Si) quantum dots are more efficient luminescence materials than crystalline silicon. This is mainly attributed to the structural disorder and relatively wide band gap energy of a-Si compared with crystalline Si, enabling nanostructured a-Si to be a viable candidate for short wavelength light emitters [7–9].

Thermoluminescence (TL) is a temperature-stimulated light emission from a system of insulating or semiconducting materials, after the removal of ionizing radiation. A plot of the light intensity as a function of temperature is known as the glow curve, which depending on the materials properties may have one or more maxima, called glow-peaks, each corresponding to an energy level of different traps [10, 11]. Various theoretical models have been proposed to describe TL processes. The simplest TL model is the one-trap-one-recombination center (OTOR) model, which is capable of describing the main features of TL processes. However, in most 'real' materials, there are several electron traps with different thermal activation energies, deep traps which retain their trapped charges during a heating cycle that empties the shallower traps, and recombination centers [12, 13]. Accordingly, a more detailed and accurate description of a TL phenomena, entails the use of more complex TL kinetic models that take into account of competitions among multiple electron traps and luminescent centers. Among such models are the interactive multiple traps system (IMTS) and non-interactive multiple traps system (NMTS). These models consist of thermally disconnected deep electron traps (TDDT), which are assumed to be thermally stable during the heating process.

An alternative version of the OTOR model is the kinetic model which consists of two/three active electron traps and a recombination center (TTOR). Size dependent TL emission and the effect of retrapping on TL peak intensities in small a-Si quantum dots (QDs) has been investigated using the TTOR model [14,15]. Their analysis show that the TL glow curve possesses two/three peaks corresponding to the two/three trapping levels, the TL intensity increases with a decrease in the size of QDs, and the simulated glow curves corresponding to each trap levels follow the second-order kinetics. Motivated with these reports, we find it interesting to study further the effect of size variation on the shape of the glow curve and TL intensity of Si nanostructures by introducing TDDT traps to the TTOR model. In this work, we investigate the effect of varying the size of spherical a-Si QDs of diameters between 3–6 nm on the TL intensity using the IMTS model. In

addition, we numerically simulated the instantaneous concentrations of carriers in the traps/center and determine the order of kinetics of the glow curves.

The paper is organized as follows: In Section 2, we present the proposed IMTS model and the corresponding rate equations. Numerical simulations, results, and discussions are displayed in Section 3. Finally, concluding remarks are given in Section 4.

2 The Thermoluminescence Kinetic Model

Consider the IMTS TL kinetic model that consists of two active electron traps (AT_1 and AT_2), one thermally disconnected deep trap (TDDT), and a luminescent center (RC), as shown in Figure 1. It is assumed that the process of traps/center filling is already attained with priori irradiations. During trap emptying (via application of heat), electrons trapped in AT_1 and AT_2 traps will be released back to the conduction band (transitions 2 and 4) when the trapped electrons absorb enough energy that is comparable to the activation energies (E_1 for AT_1) and (E_2 for AT_2). Subsequently, these thermally elevated free electrons may be released back so that they may either recombine with the holes in the RC (transition 6) yielding luminescence, or becomes retrapped at the electron traps (transitions 1, 3, 5).

For the given IMTS model, the transport of carriers during heating may be de-

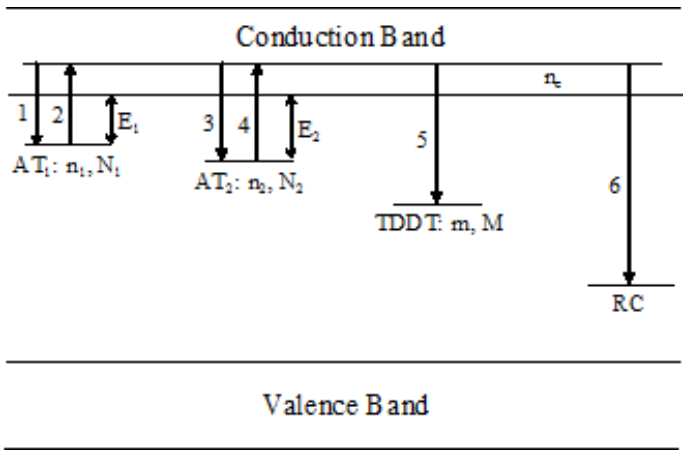

Figure 1. The IMTS model with two active electron traps AT_1 and AT_2 having activation energies E_1 and E_2, respectively; a thermally disconnected deep electron trap (TDDT); and a recombination center (RC).

scribed by the following rate equations [12, 16]:

$$\frac{dn_1}{dt} = -s_1 n_1 \exp\left(-\frac{E_1}{kT}\right) + (N_1 - n_1) n_c A_{n1}, \tag{1}$$

$$\frac{dn_2}{dt} = -s_2 n_2 \exp\left(-\frac{E_2}{kT}\right) + (N_2 - n_2) n_c A_{n2}, \tag{2}$$

$$\frac{dm}{dt} = (M - m) n_c A_m, \tag{3}$$

$$\frac{dn_h}{dt} = \frac{dn_1}{dt} + \frac{dn_2}{dt} + \frac{dm}{dt} + \frac{dn_c}{dt}, \tag{4}$$

$$\frac{dn_c}{dt} = -\frac{dn_1}{dt} - \frac{dn_2}{dt} - \frac{dm}{dt} - n_c n_h A_h, \tag{5}$$

$$I(t) = -\frac{dn_h}{dt} = n_c n_h A_h, \tag{6}$$

where I [cm^{-3}s^{-1}] is the TL intensity; N_1, N_2, and M [cm^{-3}] are the total concentrations of the AT_1, AT_2, and TDDT electron traps, respectively; n_1, n_2, and m [cm^{-3}] are the corresponding instantaneous concentrations of filled traps, n_c [cm^{-3}] is the concentration of electrons in the conduction band, n_h [cm^{-3}] is the concentration of holes in the recombination center. Also, A_{n1}, A_{n2}, and A_m [cm^3/s] are the capture coefficients for the two active and one TDDT electron traps, A_h [cm^3/s] is the capture coefficient of the recombination center, E_1 and E_2 [eV] are the activation energies of the active traps, s_1 and s_2 [s^{-1}] are the frequency factors for these traps, and k [eV/K] is the Boltzmann's constant. Note that the charge neutrality condition $n_h = n_1 + n_2 + m + n_c$ is implied in Eqs. (1)-(6).

Furthermore, in our analysis we assumed a linear heating given by

$$T(t) = T_0 + \beta t, \tag{7}$$

where T [K] is the temperature of the QDs at time t [s], T_0 is the temperature at $t = 0$, and β [Ks^{-1}] is the heating rate.

It is worthwhile noting that Eqs. (1)-(6) are coupled nonlinear first-order differential equations, which in general do not have exact analytical solutions. Often, analytical expressions for TL glow curves are obtained by imposing simplifying assumptions, such as the quasi-equilibrium conditions. In this paper, the kinetic equations will be solved numerically using MATHEMATICA 9 software.

A particular TL glow curve may be characterized by its symmetry factor (μ_g), which is defined by

$$\mu_g = \frac{\delta}{\omega}, \tag{8}$$

where $\omega = T_2 - T_1$ is the full width at half maxima, $\delta = T_2 - T_m$ is the half-width toward the fall-off side of the glow peak, T_1 and T_2 ($T_2 > T_1$) are the temperatures corresponding to half the TL intensity on either side of the peak temperature, T_m. For first- and second-order kinetics, $\mu_g = 0.42$ and 0.52, respectively. Moreover, for a particular value of μ_g, the order of kinetics, b, may be approximated by the following empirical equation [17, 18]:

$$\mu_g = C_0 + C_1 b - C_2 b^2, \tag{9}$$

where $C_0 = 0.25$ and $C_1 = 0.186$. In the analysis, we used $C_2 = 0.024$ and 0.016 for symmetrical- and asymmetrical-looking glow curves, respectively. It is worth noting that the concept of symmetry factor is applicable for TL glow curves where the numerically simulated TL curves possess isolated broad peaks [17].

Table 1. Approximate values of the size dependent radiative recombination rate of electron in the conduction band to recombine with hole in the RC of a-Si QDs. [4]

Diameter, d [nm]	Radiative recombination rate, γ_r [s^{-1}]
3	7.0×10^6
4	3.0×10^6
5	9.0×10^5
6	4.0×10^5

3 Results and Discussions

For numerical computation of TL curves by using the set of Eqs. (1)-(6), the initial concentrations of carriers n_{10}, n_{20}, and m_0 in the traps AT_1, AT_2, and TDDT, respectively, are computed according to a saturating exponential function in which the filling rate constant is assumed to be proportional to the corresponding trapping coefficients [13, 17]. Typical values of the retrapping and recombination coefficients vary between 10^{-10}–10^{-5} cm^3s^{-1} [12]. Accordingly, neglecting possible corrections associated with confinement, we choose $A_{n1} = A_{n2} = A_m = 10^{-9}$ cm^3/s. The radiative recombination rate (γ_r) and the recombination coefficient are related by $A_h = \gamma_r n_h^{-1}$ [10]. Hence, using the values of γ_r tabulated in Table 1, the size dependent recombination coefficients are calculated to be $A_h = (3.50,\ 1.50,\ 0.45,\ 0.20) \times 10^{-8}$ cm^3s^{-1}, for the QDs of size $d = (3,\ 4\ ,5,\ 6)$ nm, respectively. Below, we simulated the various TL parameters of interest using theses values.

Figures 2 and 3 show the concentration of electrons in the active electron traps AT_1 and AT_2, respectively, as a function of temperature. The concentration of electrons in the traps AT_1 ($E_1 = 0.65$ eV) decreases as the temperature increases, almost independent of the QDs size. Furthermore, it is seen that

$n_1(T)$ are almost independent on the size of the QDs, contrary to that reported in Refs. [14, 15], which was obtained using the TTOR model. On the other hand, as the temperature increases, the concentration of electrons in the traps AT_2 ($E_2 = 0.80$ eV) initially increases just after a temperature of about $50°$C, until it reaches a peak value at about $110°$C, and then decreases thereafter be-

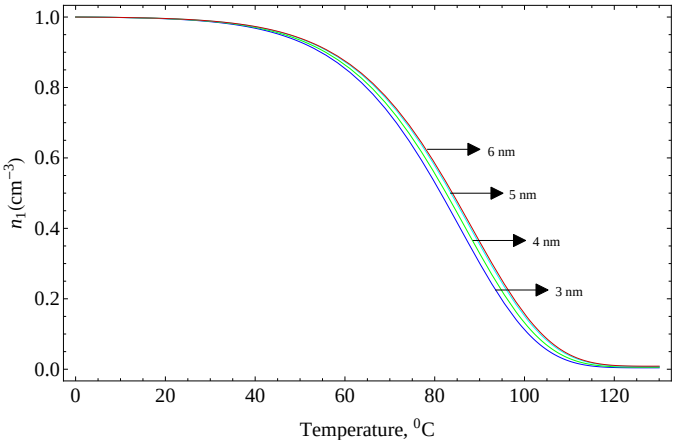

Figure 2. The normalized concentration of trapped electrons in the traps AT_1 as a function of temperature for four different quantum dot sizes. The values used for the plots are: $N_1 = N_2 = M = 10^{16}$ cm^{-3}, $n_{10} = n_{20} = m_0 = 2 \times 10^{14}$ cm^{-3}, $A_{n1} = A_{n2} = A_m = 10^{-9}$ cm^{3}s^{-1}, $\beta = 1$ Ks^{-1}, $E_1 = 0.65$ eV, $E_2 = 0.80$ eV, and $s_1 = s_2 = 10^8$ s^{-1}.

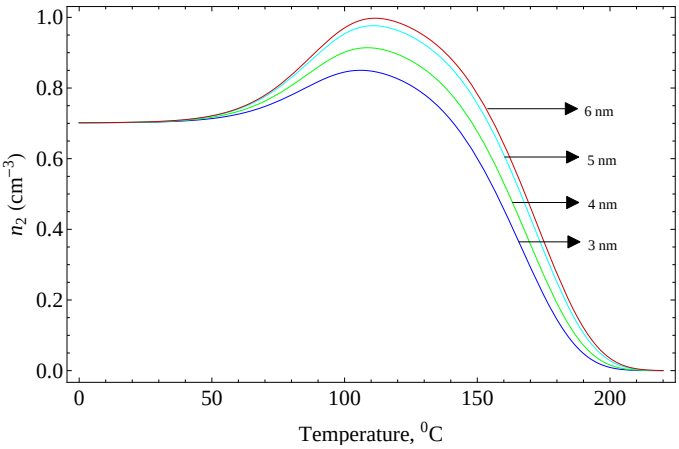

Figure 3. The normalized concentration of trapped electrons in the trap AT_2 ($E_2 = 0.80$ eV) as a function of temperature; with the same parameters as in Figure 2.

coming zero just above 220°C. Note that the activation energy of the traps AT_1 is less than that of the traps AT_2 ($E_1 < E_2$), which means that electrons initially trapped during irradiation in AT_1 are released into the conduction band before those trapped in AT_2 are activated. This accounts for the initial increase in n_2 (between 50–110°C) that some of the electrons released from traps AT_1 are retrapped in AT_2 thereby increasing the value of n_2.

As shown in Figure 4, the instantaneous concentration of electrons $m(T)$ in the TDDT traps increases with an increase in temperature until about 210°C and then reach saturation values above $\approx$ 210°C. Moreover, the saturation values are seen to increase with an increase in the size of the QDs. This may be explained in terms of the difference in the recombination coefficients, A_h. That is, as the size of the QDs increases, A_h decreases which in turn means lesser number of electrons from the active electron traps reaching the RC and producing TL emission; instead many more electrons are more likely to be retrapped in the TDDTs before reaching the RC. Also note that when the temperature is between 100°C and 130°C, the increase in $m(T)$ is small (plateau), which may be accounted with the fact that trap AT_1 is on the verge of being fully emptied, while electrons in trap AT_2 are not yet sufficiently activated, and hence the number of electrons to be retrapped by the TDDT traps is reduced significantly.

Figure 5 shows the variation of concentrations of electrons in the conduction band as a function of temperature for the QDs of diameters between 3–6 nm. It is observed that the concentration of electrons in the conduction band possess two sets of peaks in the vicinity of $T = 85$°C and $T = 165$°C corresponding to the trap levels E_1 and E_2, respectively. Moreover, it is seen that when the quantum dots sizes increase, $n_c(T)$ also increase. It is because that the recombination

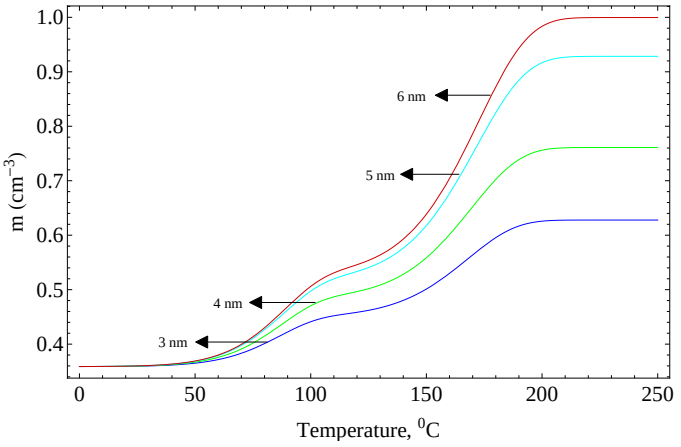

Figure 4. The normalized concentration of trapped electrons in the TDDT traps as a function of temperature; with the same parameters as in Figure 2.

lifetime, which is the mean time spent by an electron in the conduction band, is large for QDs of larger size. It means that free electrons in the conduction band spend more time before recombining with the holes in the RC centers for QDs with larger size than those with small size. Since A_h represents the recombination transition coefficient for electrons in the conduction band to recombine with holes in the luminescent centers, small A_h (larger QD size) means slow rate of recombination with the holes, with the electrons spending more time in the conduction band, and vice versa.

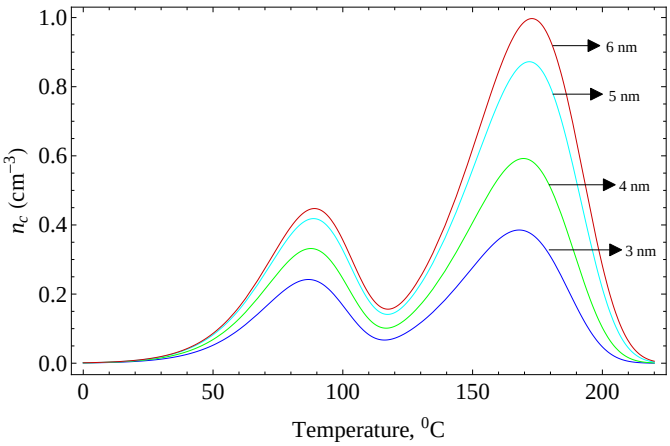

Figure 5. The normalized concentration of electrons in the conduction band versus temperature; with the same parameters as in Figure 2.

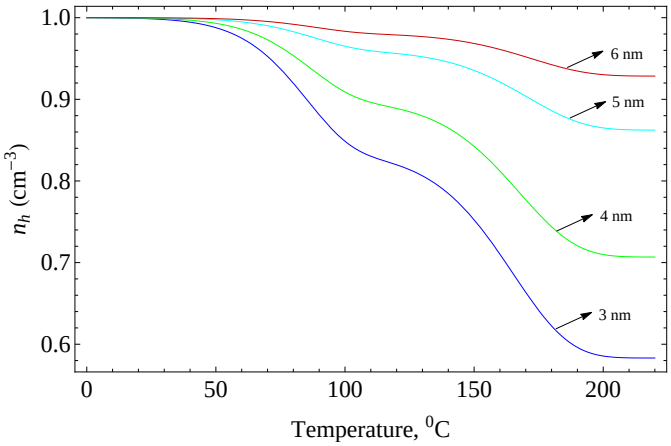

Figure 6. The normalized concentration of holes in the recombination center as a function of temperature; with the same parameters as in Figure 2.

Figure 6 depicts the instantaneous concentration of holes in the RC as a function of temperature. Recall that the charge neutrality condition dictates that $n_h(T) = n_1(T) + n_2(T) + m(T) + n_c(T)$ and since initially (just before starting the heating process), $n_c(0) = 0$ so that its peak value is $n_h(0) = n_1(0) + n_2(0) + m(0) = 6 \times 10^{14}$ cm^{-3} (or, the normalized peak value of $n_h(0) = 1$). As the temperature increase, $n_h(T)$ decrease until about 210°C and thereafter reach saturation values. It is seen that the decrease in $n_h(T)$ becomes very rapid with a decrease of the QDs size. In addition, the saturation values also increases as the QDs sizes increases, which means that the number of electrons released from the conduction band and end up being retrapped in the TDDT traps before reaching the RC increases with an increase in size resulting to a corresponding reduction in the intensity of the TL signal (see Figure 7). This result is consistent with the fact that as the size of the QDs increases, the recombination coefficient (A_h) decreases which in turn means lesser number of electrons from the active electron traps AT_1 and AT_2 reach the RC resulting to a relatively weak TL emission; instead many more electrons are retrapped in the TDDTs before reaching the RC as it is evident from Figure 4.

At this point, it is worth noting that the results obtained in Figures 2–6 cannot be realized using experimental techniques. However, the numerical method enables us to observe how the concentration of electrons and holes in the system behaves as a function of temperature and the size of the quantum dots.

Figure 7 shows the intensity of the TL emission as a function of temperature. The two sets of glow peaks around $T_m = 85$°C and $T_m = 165$°C correspond to the trap levels $E_1 = 0.65$ eV and $E_2 = 0.80$ eV, respectively. It is observed that when the quantum dots size decreases, the intensity of the TL emission

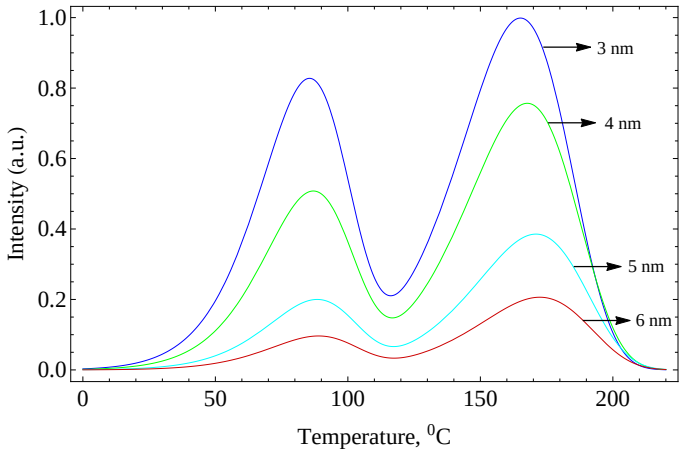

Figure 7. The TL intensity versus temperature for the same values as in Figure 2.

increases, while the peak temperature almost remains constant independent of the size of the QDs (with maximum $\Delta T_m \approx 7°\text{C}$ for both set of peaks). The enhancement of the TL signal with a decrease of QDs size is due to the quantum confinement effect. This is because that the confinement effect causes an increase in the number of surface states thereby resulting to more holes and electrons to be accessible for the TL recombination, and the wave functions of the electrons and holes in the QDs are overlapped effectively, resulting to an increase of their radiative recombination rate [3, 4] as well as the enhancement of the TL emission.

Notice that the simulated TL glow curve has a very similar shape to that of the instantaneous concentration of electrons in the conduction band. The peak values of the TL intensity occur at the same temperature as that of $n_c(T)$, shown in Figure 5. Also, it is worthwhile to note that the temperature ($\sim 210°\text{C}$) at which $m(T)$ saturates coincides with the value, where the TL glow curves ends (see Figure 7).

Setting $M = m_0 = 0$ ($A_m = 0$) in Eq. (3), the IMTS model becomes the TTOR model reported in Ref. [14]. The corresponding graph of the TL intensity as a function of temperature are depicted in Figure 8, with the same parameters as that used for the IMTS model. Similar to the IMTS model, the glow curves possess two sets of peaks: the first around $T_m = 90°\text{C}$ and the second above $T_m = 190°\text{C}$, corresponding to the trap levels E_1 and E_2, respectively. It is observed that when the quantum dots size decrease, the intensity of the TL intensity increase; while the peak temperatures shift towards higher values with an increase in the QDs size. Further, close observation of Figure 8 and Table

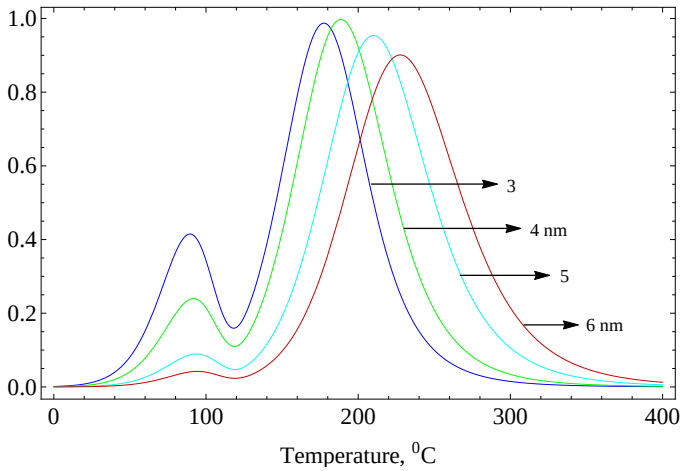

Figure 8. The TL intensity versus temperature for $M = m_0 = 0$ (TTOR model). The other parameter values are the same as that in Figure 2.

2 shows that the widths of the glow curves become broader and broader (maximum $\Delta\omega = 21.3°$C) with an increase in the QDs size. It is well known that the size of the width is associated with the dissipation (scattering) in a material medium [20]. Consequently, as the size of the quantum dots increases, collision between the atoms increases thereby increasing the dissipation which is reflected via an increased broadening of the width of the glow curve.

Table 2. The calculated values of the symmetry factor μ_g and order of kinetics b for the simulated glow peaks corresponding to $E_2 = 0.80$ eV.

Model	Trap	d [nm]	T_m [°C]	ω [°C]	δ [°C]	μ_g	b
IMTS	AT_2	3	165.5	49.5	21.2	0.428	1.052
		4	167.7	49.7	21.2	0.427	1.046
		5	170.6	49.6	21.4	0.432	1.079
		6	172.3	49.7	21.3	0.429	1.059
TTOR	AT_2	3	177.1	66.2	33.8	0.511	1.840
		4	188.0	71.1	37.4	0.526	2.000
		5	208.5	79.7	43.1	0.541	2.175
		6	227.2	87.5	46.7	0.534	2.091

Furthermore, the numerically computed symmetry factor, order of kinetics, and other relevant parameters corresponding to the glow peaks (corresponding to $E_2 = 0.80$ eV) of Figures 7 and 8 are presented in Table 2. The results show that for the IMTS model, the peaks in the vicinity of 165°C follow almost first-order kinetics with $\mu_g = 0.427$–0.432 and $b = 1.052$–1.079; while the peaks for the TTOR model located between 177–227°C follow approximately second-order kinetics with $\mu_g = 0.511$–0.541 and b between 1.840–2.175. The result is consistent with the fact that irrespective of the presence of retrapping, the IMTS model lead to first-order looking glow curves due to the large number of electrons in the TDDT traps [19]. Also, it is worth noting that the concept of symmetry factor is applicable for TL glow curves, where the numerically simulated TL glow curves possess isolated broad peak [17].

4 Conclusions

We studied the effect of size variation on TL emission of a-Si QDs using the IMTS model. The size effect is taken into account by introducing the size dependent recombination probability coefficient. We find that as the size of the quantum dots decrease, the intensity of the TL signal increase. Further, comparison of the results for the IMTS and TTOR models, i.e., Figures 7 and 8 as well as Table 2, show that: (i) the IMTS model lead to first-order looking glow curves with $\mu_g \sim 0.42$, while the glow curve for the TTOR model resembles second-order with $\mu_g \sim 0.52$, and (ii) in the TTOR model, the peak temperature shifts towards higher values and the widths of the glow curves gets broader and

broader with an increase in the QDs size, whereas it is almost independent of size for the IMTS model. We believe that the results may be used in the design and fabrication of devices for TL applications employing compounds enriched with silicon.

References

[1] A. Rastar, M. E. Yazdanshenas, A. Rashidi, and S. M. Bidoki (2013) *J. Eng. Fib. Fabri.,* **8** 2.

[2] S. A. Cabanas-Tay, L. Palacios-Huerta, M. Aceves-Mijares, A. Coyopol, S. A. Perez-Garcia, L. Licea-Jimenez, C. Dominguez, and A. Morales-Sanchez (2016) *Luminescence - An Outlook on the Phenomena and their Applications,* InTECH, Ch. 8, pp. 159-187.

[3] J. A. Rodriguez, M. A. Vasquez-Agustin, A. Morales-Sanchez, and M. Aceves-Mijares (2014) *J. Nanomater.* Vol. 2014, 409482.

[4] N. M. Abdul-Ameer and M. C. Abdulrida (2011) *J. Mod. Phys.* **2** 1530.

[5] S. K. Ghoshal, G. A. Desalegn, E. A. Abebe, H. S. Tewari, and P. K. Bajpai (2009) *J. Int. Acad. Phys. Sci.* **13(2)** pp. 105-116.

[6] C. -C. Tu, Q. Zhang, L. Y. Lin, and G. Cao (2012) *Opt. Expr.,* **20(1)** pp. A69-A74.

[7] H. S. Kwach, Y. Sun, Y. H. Cho, N. M. Park, and S. J. Park (2003) *Appl. Phys. Lett.* **83(14)** 2901.

[8] N. M. Park, C. J. Choi, T. Y. Seong, and S. J. Park (2001) *Phys. Rev. Lett.* **86(7)** 1355.

[9] N. M. Park, T. S. Kim, and S. J. Park (2001) *Appl. Phys. Lett.* **78(17)** 2575.

[10] S. W. S. Mckeever, *Thermoluminescence of Solids,* Cambridge University Press, Cambridge.

[11] C. Furetta (2003) *Handbook of Thermoluminescence,* World Scientific Publishing Ltd.

[12] V. Pagonis and G. Kitis (2012) *Phys. Status Solidi B,* pp. 1-12.

[13] C. M. Sunta (2015) *Unraveling Thermoluminescence,* Springer, Vol. 202.

[14] N. Gemechu, T. Senbeta, B. Mesfin, and V. N. Mal'nev (2017) *Ukr. J. Phys.* **62** 2.

[15] N. G. Debelo, F. B. Dejene, V. N. Mal'nev, T. Senbeta, B. Mesfin, and K. Roroa (2016) *Acta Phys. Pol,* **129** 3.

[16] V. Pagonis, G. Kitis, and C. Furetta (2006) *Numerical and Practical Exercises in Thermoluminescence,* Springer, New York.

[17] M. Karmakar, S. Bhattacharyya, A. Sarkar, P. S. Mazumdar, and S. D. Singh (2017) *Radiat. Prot. Dosi.* **175(4)** 493.

[18] S. J. Singh, M. Karmakar, M. Bhattacharya, S. D. Singh, W. S. Singh, and S.K. Azharuddin (2012) *Ind. J. Phys.* **86** 113.

[19] K. Ankama Rao, S. P. Niyaz, N. V. Poornachandra Rao, and K. V. R. Murthy (2011) *Arc. Phys. Res.* **2(4)** 89.

[20] Challa S. S. R. Kumar (2013) *UV-VIS and Photoluminescence Spectroscopy for Nanomaterials Characterization,* Springer-Verlag, Berlin.